Molecular Phylogenetics and Evolution xxx (xxxx) 107347

Contents lists available at ScienceDirect

Molecular Phylogenetics and Evolution

journal homepage: www.elsevier.com/locate/ympev

Independent evolutionary transitions to pueriparity across multiple timescales in the viviparous genus *Salamandra*

Kevin.P. Mulder[a,b,c,d,*], Lucía Alarcón-Ríos[a,b,e], Alfredo G. Nicieza[e,f], Robert C. Fleischer[d], Rayna C. Bell[c,g], Guillermo Velo-Antón[a,b,h,*]

[a] CIBIO, Centro de Investigação em Biodiversidade e Recursos Genéticos, InBIO Laboratório Associado, Campus de Vairão, Universidade do Porto, 4485-661 Vairão, Portugal
[b] BIOPOLIS Program in Genomics, Biodiversity and Land Planning, CIBIO, Campus de Vairão, 4485-661 Vairão, Portugal
[c] Department of Vertebrate Zoology, National Museum of Natural History, Smithsonian Institution, 1000 Constitution Avenue NW, Washington, DC 20560, USA
[d] Center for Conservation Genomics, Smithsonian Conservation Biology Institute, National Zoological Park, 3001 Connecticut Avenue NW, Washington, DC 20008, USA
[e] Departamento de Biología de Organismos y Sistemas, Universidad de Oviedo UO, Oviedo, Spain
[f] Biodiversity Research Institute (IMIB), University of Oviedo-Principality of Asturias-CSIC, 33600 Mieres, Spain
[g] Herpetology Department, California Academy of Sciences, 55 Music Concourse Drive, San Francisco, CA 94118, USA
[h] Universidade de Vigo, Grupo GEA, Departamento de Ecoloxía e Bioloxía Animal, Vigo, Spain

ARTICLE INFO

Keywords:
Amphibians
Ancestral state reconstruction
Reproductive mode
Sequence capture
Viviparity

ABSTRACT

The ability to bear live offspring, viviparity, has evolved multiple times across the tree of life and is a remarkable adaptation with profound life-history and ecological implications. Within amphibians the ancestral reproductive mode is oviparity followed by a larval life stage, but viviparity has evolved independently in all three amphibian orders. Two types of viviparous reproduction can be distinguished in amphibians; larviparity and pueriparity. Larviparous amphibians deliver larvae into nearby ponds and streams, while pueriparous amphibians deliver fully developed juveniles and thus do not require waterbodies for reproduction. Among amphibians, the salamander genus *Salamandra* is remarkable as it exhibits both inter- and intraspecific variation in the occurrence of larviparity and pueriparity. While the evolutionary relationships among *Salamandra* lineages have been the focus of several recent studies, our understanding of how often and when transitions between modes occurred is still incomplete. Furthermore, in species with intraspecific variation, the reproductive mode of a given population can only be confirmed by direct observation of births and thus the prevalence of pueriparous populations is also incompletely documented. We used sequence capture to obtain 1,326 loci from 94 individuals from across the geographic range of the genus, focusing on potential reproductive mode transition zones. We also report additional direct observations of pueriparous births for 20 new locations and multiple lineages. We identify at least five independent transitions from the ancestral mode of larviparity to pueriparity among and within species, occurring at different evolutionary timescales ranging from the Pliocene to the Holocene. Four of these transitions occurred within species. Based on a distinct set of markers and analyses, we also confirm previous findings of introgression between species and the need for taxonomic revisions in the genus. We discuss the implications of our findings with respect to the evolution of this complex trait, and the potential of using five independent convergent transitions for further studies on the ecological context in which pueriparity evolves and genetic architecture of this specialized reproductive mode.

1. Introduction

The ability to bear live offspring, viviparity, is a remarkable adaptive trait found across the tree of life, with at least 150 independent transitions to viviparity in vertebrates (Blackburn, 2015; Gower et al., 2008; Helmstetter et al., 2016; Reynolds et al., 2002). Viviparity is associated with better protection of offspring, diversification, and the exploitation of new ecological habitats (Helmstetter et al., 2016;

* Corresponding authors at: CIBIO/InBIO, Research Center in Biodiversity and Genetic Resources, Rua Padre Armando Quintas 7, Campus Agrário de Vairão, 4485-661 Vairão, Portugal.
E-mail addresses: kmulder@cibio.up.pt (Kevin.P. Mulder), guillermo.velo@uvigo.es (G. Velo-Antón).

https://doi.org/10.1016/j.ympev.2021.107347
Received 21 June 2021; Received in revised form 21 October 2021; Accepted 3 November 2021

Pincheira-Donoso et al., 2013; Recknagel et al., 2021; Wake, 2015). The evolution of viviparity can thus have profound effects on the evolutionary trajectory of a given lineage. Within amphibians viviparity has evolved independently in all three amphibian orders, and two types of viviparous reproduction can be distinguished; larviparity and pueriparity (sensu Greven, 2003). This variation in viviparous strategies, allow us to understand and test the evolutionary and ecological context of viviparous reproduction using amphibians as a model system.

Within amphibians the ancestral reproductive mode is oviparity; following the delivery and external fertilization of eggs, the young hatch as larvae and later undergo metamorphosis to their adult form (Wake, 1982). Larviparity, which is documented in four salamander species (Buckley, 2012) and in one frog species (Iskandar et al., 2014), is characterized by internal fertilization, an incubation period, and subsequent delivery of larvae into nearby waterbodies (Greven, 2003). This reproductive strategy is hypothesized to help reduce egg predation and increase fecundity (Greven, 2003). By contrast, pueriparity, in which species skip this larval stage and females deliver fully developed juveniles, is relatively common in caecilians (~34/214 species), and rare in anurans (16/7,164) and urodeles (11/742; Frost, 2021; Buckley, 2012; Sandberger-Loua et al. 2017). Hypotheses for the evolution of pueriparity include that it is an evolutionary response to xeric climatic conditions and a corresponding lack of suitable water bodies for larval delivery (Beukema et al., 2010; García-París et al., 2003; Liedtke et al., 2017; Velo-Antón et al., 2012), or alternatively, that it is a response to high larval predation and natural larval loss (Greven, 2003). Within salamanders, all known cases of larviparity and pueriparity are restricted to two sister genera; *Lyciasalamandra* in which all seven species are pueriparous, and *Salamandra* which includes six species with multiple representatives of both modes. This provides a unique comparative framework to investigate the genetic architecture and convergent evolution of larviparity and pueriparity.

The genus *Salamandra* is remarkable as it exhibits both inter- and intraspecific variation in the occurrence of larviparity and pueriparity. The two alpine species *S. atra* and *S. lanzai* are strictly pueriparous, the species *S. infraimmaculata* in the Eastern Mediterranean and *S. corsica* on the Mediterranean island of Corsica are larviparous, and the widespread species *S. salamandra* in Europe and *S. algira* in North Africa show intraspecific variation in reproductive mode (Fig. 1 & Fig. 2). Although phenotypic plasticity by either epigenetic inheritance or early life-stage imprinting have not been investigated, the delivery of larvae versus juveniles does not appear to be plastic as sexually mature females in controlled lab environments maintain their respective reproductive mode (Velo-Antón et al., 2007, 2015) and heterochronic changes occur in the early stages of embryonic development, confirming that pueriparity is not caused by the retention of larvae until metamorphosis (Buckley et al., 2007). *Salamandra* are thus a compelling system to test comparative evolutionary and ecological hypotheses related to the transition to pueriparity. Although the evolutionary relationships among *Salamandra* species and subspecies have been the focus of several studies (Burgon et al., 2021; Rodríguez et al., 2017), our understanding of how often and when transitions between modes occurred are not yet clear due to a lack of sampling along transition zones. Furthermore, in species with intraspecific variation in reproductive mode, the mode of a given population can only be confirmed by direct observation of births and thus the prevalence of pueriparous populations is incompletely documented.

Several species-level topologies have been proposed for *Salamandra* (Steinfartz et al., 2000; Veith et al., 1998; Vences et al., 2014), but the most recent and complete genus level datasets points to a single transition to pueriparity in *S. atra/S. lanzai* and independent transitions for both *S. salamandra* and *S. algira* (Rodríguez et al., 2017; Dinis et al., 2019). Recent phylogenomic analyses using ddRAD data from across the taxonomic and geographic breadth of the genus *Salamandra* strongly supported species-level relationships and clarified subspecies relationships within *S. algira* and *S. salamandra*, indicating paraphyletic positions of some *S. salamandra* subspecies which require further investigation (Burgon et al., 2021). However, this phylogenomic study did not specifically account for the reproductive shift in this group due to the lack of representatives from some pueriparous localities and comprehensive sampling across the transition zones. Within *S. salamandra*, pueriparity has been described in three of the ten main subspecies. *Salamandra s. bernardezi* in northern Spain (Fig. 1) is considered pueriparous (Alarcón-Ríos et al., 2020b; Buckley et al., 2007; Velo-Antón et al., 2015), but genetic diversity and divergence within the subspecies is very high (Beukema et al.,

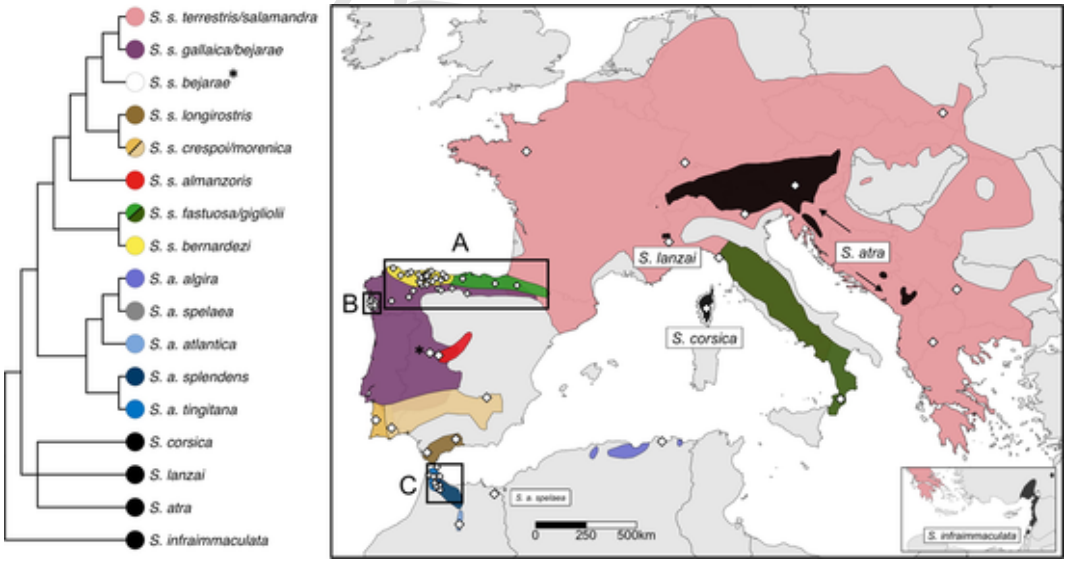

Fig. 1. Schematic of the phylogenetic relationships of species and subspecies (*S. salamandra* and *S. algira*) based on results from this study, and the ranges of all six *Salamandra* species and major subspecies of *S. salamandra* and *S. algira*. Location of the genetic samples included in this study are indicated by white diamonds. The range of *S. infraimmaculata* is presented in an inset due to its disjointed location in the Eastern Mediterranean and *S. a. spelaea* is indicated by a label due to its small distribution. Both *S. atra* and *S. lanzai* are strictly pueriparous and *S. corsica* and *S. infraimmaculata* are strictly larviparous. *Salamandra salamandra* and *S. algira* show intraspecific variation in reproductive mode centered around populations in box A, B and C which are described in more detail in Fig. 2.

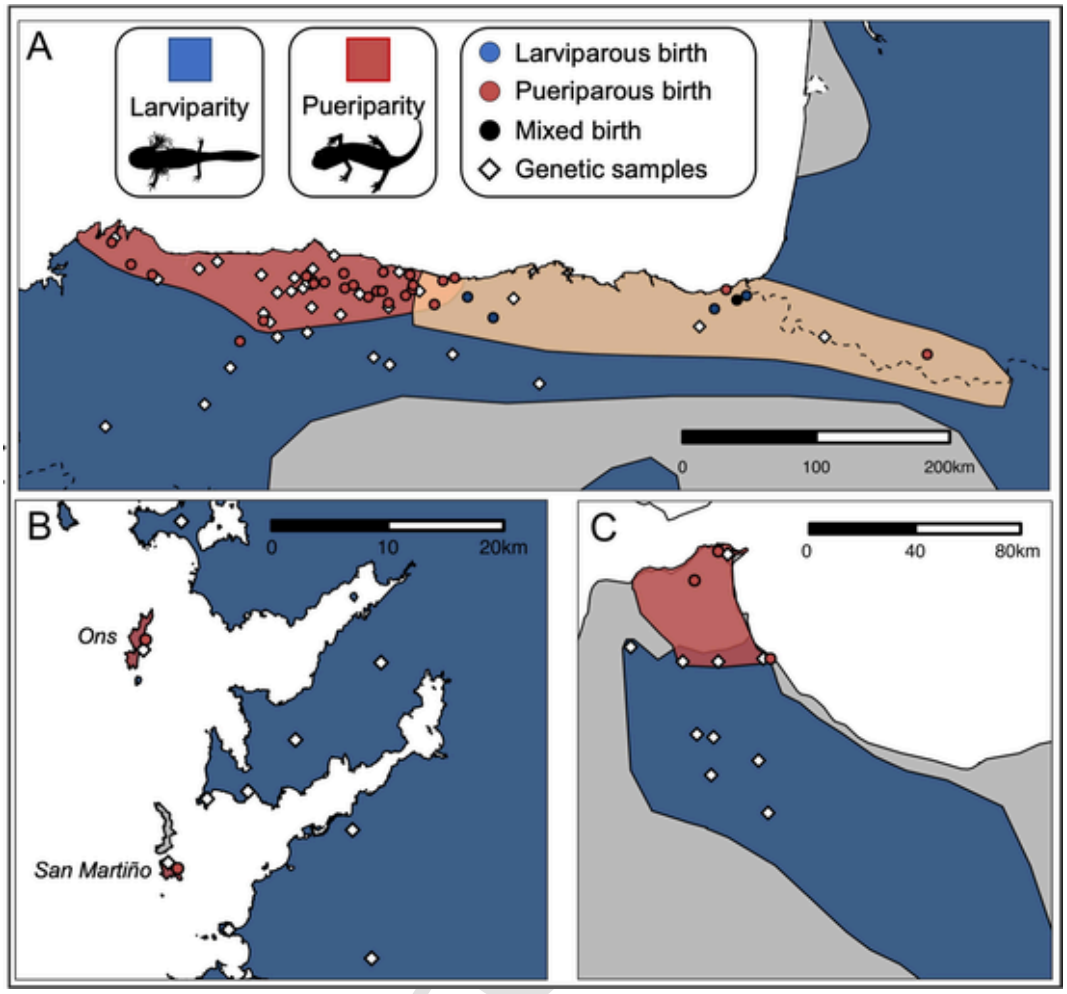

Fig. 2. Sampling localities across three of our focal areas, see Fig. 1 for location of the insets. Red indicates putative extent of pueriparity, blue larviparity, and in orange is the range of *S. s. fastuosa* for which both reproductive modes have been recorded. Genetic samples indicated by white diamonds, confirmed pueriparous births by red dots, larviparous births by blue dots and populations with mixed births by black dots. *Salamandra salamandra* sampling localities in (A) northern Iberia for *S. s. bernardezi* (red), *S. s. fastuosa* (beige) and *S. s. gallaica* and relatives (blue), (B) Galicia, NW Spain for *S. s. gallaica* and (C) *S. algira* localities in northern Morocco. (For interpretation of the references to color in this figure legend, the reader is referred to the web version of this article.)

2016; Lourenço et al., 2019), and for large parts of its range there are no direct observations of reproductive mode (Fig. 2A). *Salamandra s. fastuosa*, found to the east of *S. s. bernardezi* (Fig. 1 and Fig. 2A) in northern Spain, includes both larviparous and pueriparous populations (Uotila et al., 2013), and pueriparity in this subspecies has been hypothesized to be due to introgression from pueriparous *S. s. bernardezi* (Fig. 2A; García-París et al., 2003). Additionally, two insular populations of *S. s. gallaica* are pueriparous (Fig. 2B; Velo-Antón et al., 2007, 2012, 2015). The island populations are genetically distinct from adjacent mainland populations based on microsatellite markers (Lourenço et al., 2018b; Velo-Antón et al., 2012); however, the evolutionary relationships among these populations are not fully understood. Finally, within *S. algira tingitana* one mitochondrial lineage is documented as pueriparous while a second one is both larviparous and pueriparous, which may be due to introgression events across their contact zone (Fig. 2C; Dinis et al., 2019; Dinis and Velo-Antón, 2017).

We aim to clarify the evolutionary history of *Salamandra,* with a special emphasis on pueriparous populations and their neighboring larviparous populations, to determine the number and timing of transitions to pueriparity within the genus. We performed sequence capture on 1,326 loci of 94 individuals from across the geographic range of the genus, including all subspecies and pueriparous lineages within *S. salamandra* and *S. algira*, to estimate and date phylogenetic relationships. We also assessed the reproductive mode across *S. s. bernardezi* and *S. s. fastuosa* by collecting data on the reproductive output of females from 20 localities across the *S. s. bernardezi* range and neighboring areas, and summarizing all the pueriparous births previously reported in the literature for these subspecies (Fig. 2A; Table S2). This study clarifies the number and timing of independent transitions to pueriparity across the genus, increases the known current geographic and phylogenetic extent of larviparity and pueriparity in *Salamandra,* and sets up the basis to further test the evolutionary and ecological context of viviparous reproduction using amphibians as a model system.

2. Material and methods

2.1. Field sampling and reproductive mode scoring

We collected toe-clips for genomic analyses from across the range of *Salamandra* (Fig. 1; Table S1), focusing in and around intraspecific lineages for which the reproductive mode was known based on previous and current work: (a) *S. s. bernardezi*; (b) insular-mainland populations of *S. s. gallaica*, and (c) *S. a. tingitana* (Fig. 2).

Separately, we also collected pregnant salamanders during the reproductive periods between 2015 and 2018 from 20 localities that over-

lap with the genetic sampling across the ranges of *S. s. bernardezi* (N = 35) and *S. s. fastuosa* (N = 2) (Velo-Antón et al., 2021), to assess their reproductive modes (see Table S2). We transported females to laboratory facilities at the University of Oviedo and placed them in individual terraria (60 × 30 × 40 cm; L × W × H) equipped with a coconut fiber substrate, a container with water, moss, and shelters (bricks or barks). We fed them ad libitum twice a week with crickets and flour worms and collected tail-tips from females for mtDNA barcoding. Barcoding was used to ensure the samples for reproductive mode assessment covered the same phylogenetic diversity as sampled in the sequence capture dataset. After parturition, we returned them, together with their offspring, to the place of capture.

2.2. Sequence array design

The majority of loci in the sequence array were based on variable regions found in the 3,070 orthologous loci identified for the *Salamandra* reference transcriptome (Rodríguez et al., 2017). To identify variable regions, we mapped separately collected RNAseq reads (Mulder et al., in prep; NCBI Bioproject PRJNA385088) back to the orthologous loci and identified 1,287 unlinked Single Nucleotide Polymorphisms (SNPs) at a variety of phylogenetic levels (between species, between subspecies and inter- and intrapopulation levels). Sequences of ~ 175 base pairs (bps) were extracted around these SNPs, targeting a total of 201,026 bps (Supplemental file S1).

We added an additional 39 nuclear loci available for *Salamandra* from GenBank (see Table S3 for a summary), selecting sequences between 300 and 1,540 bps, including longer fragments for more informative loci, for a total of 20,198 bps. To compare the samples to the barcoded individuals with confirmed births (Section 2.1), we also included a 130 bp fragment for the mitochondrial gene cytochrome *B* (CytB). Mitochondrial DNA enriches at higher efficiency during sequence capture than nuclear DNA, so at this length we can extract the target sequence plus flanking areas, resulting in an alignment that is comparable in size to previous CytB datasets collected by Sanger sequencing.

Total sequence array size was 1,326 loci and 221,224 bps (Supplemental Information file S1). Following a quality control pipeline by Arbor Biosciences (Ann Arbor, MI, USA) to filter the probes for GC-content, repetitive elements and hybridization temperature, a total of 5,077 tiled baits of 90 bp each were designed across these sequences, tiled at ~ 5X to increase the sequence capture efficiency.

2.3. Laboratory methods

2.3.1. Genomic library preparation

We extracted genomic DNA from 94 salamander toe-clips (Table S1) using a high-salt extraction protocol (Gentra Puragene reagents; Qiagen, Chatsworth, CA, USA), and eluted the extractions in 100 μl of EB buffer. Following quantification with the Qubit 2.0 dsDNA HS Assay kit (Invitrogen, Carlsbad, CA, USA), we sheared 800 ng of DNA to a mean size range of ~ 300 bps with 20 cycles of sonication on the Bioruptor Pico (Diagenode, Liège, Belgium) in 0.2 ml tubes at intervals of 30 sec on/30 sec off with a short spin after the first set of 10 cycles.

Sheared DNA was prepared for sequencing following the BEST 2.0 protocol (Carøe et al., 2018) with dual indexed 7 bps adapters (Kircher et al., 2012). We added stubby adapters at a 30× excess during ligation, and amplified half of the final solution using 9–10 cycles of indexing PCR. We pooled samples equimolarly in groups of six aiming for a total input of 3000 ng per pool, and ran a subset of pools on the TapeStation 2100 using the High Sensitivity DNA Assay (Agilent technologies, Santa Clara, CA, USA) at several stages of the protocol.

2.3.2. Sequence capture and sequencing

Pooled libraries and baits were hybridized for 36 h following the MyBaits v.3 protocol with twice the recommended amount of cot-1 blocker. Following stringent washes, we re-amplified the pools in two separate PCR reactions for 9–13 cycles. A final pool was prepared for paired end 150 bp sequencing on part of an Illumina NovaSeq S4 run at the UC Davis Genome Center. We pooled samples equimolarly, sourcing DNA from both PCR reactions but with a preference for the reaction with the least number of cycles to reduce the number of PCR duplicates in sequencing.

2.3.3. Barcoding of pregnant females with cytochrome B

We extracted genomic DNA from tissue samples of collected pregnant females using the EasySpin Genomic DNA Tissue Kit (Citomed, Lisboa, Portugal), following the manufacturer's protocol. We amplified a CytB fragment of ca. 1100 bp, following the protocol described in (Beukema et al., 2016) and outsourced DNA sequencing to Genewiz Inc. (Leipzig, Germany).

2.4. Bioinformatic processing

The majority of loci we targeted were based on transcriptome cDNA sequences that do not include introns and thus are not an accurate genomic reference for mapping capture data. To split up the putative exons within a locus we applied the IEB-finder pipeline that identifies intron–exon boundaries by means of mapping scores (Deleury et al., 2019). In short, gDNA reads are mapped against a cDNA reference using a local mapper (bwa mem; Li and Durbin, 2009) and the parts of the read that represent the intron are soft-trimmed. IEB-finder scans a bam file to identify regions that have above average soft-trimming compared to the surrounding region and identifies them as putative exon–intron boundaries (Deleury et al., 2019). We used a representative pool of 12 samples of *S. salamandra* to run the IEB-finder pipeline (parameters -e 0 -c 10 -x 30) and split up our loci into separate exons for all identified boundaries.

We ran the new reference through the SECAPR pipeline (Andermann et al., 2018), using the same 12 samples to identify potential paralogs and duplicate loci. In short, reads were quality filtered and assembled individually using abyss (-k 90; Birol et al. 2009), and the resulting assemblies were compared to the reference by means of reciprocal blast using LASTZ (--min-coverage 80, --min-identity 80; Harris 2007). We manually examined loci that were found to either contain potential paralogs (multiple contigs hitting the same locus), or duplicate loci (one contig hitting two loci). Duplicate loci were often found to be due to short introns/indels that caused IEB-finder to split the locus up, but in which flanking parts of the sequence reads were long enough to bridge this gap and form one assembled contig. We combined these loci into one locus for an updated reference that included the intron, and removed any indels from the updated reference sequence. We examined all loci identified as paralogs by SECAPR to determine if they could unequivocally be split into two loci by shifting or extending the reference sequence. If there was a clear distinction along part of the alignment (~20% sequence dissimilarity) we extended the reference locus to this section and extracted two separate sequences as input for the updated reference. If the paralogs were too similar or the SECAPR pipeline still identified the updated locus as a paralog, we removed the locus.

We ran the updated reference (Supplemental Information file S2) through the SECAPR pipeline again, using all 94 individuals but increasing the LASTZ threshold (--min-coverage 90, --min-identity 90). Following the remapping step, we ran GATK 3.8.1 (McKenna et al., 2010) across all bam files to call high quality SNPs using information from all samples. We used the EMIT-ALL-SITES to also keep non-variable sites. This combined strategy allowed us to include all available evidence to determine SNP quality, while still keeping non-variable sites for phylogenetic analyses. Following strict filtering of low-quality and low coverage SNPs, indels and paralogous loci, alignments were extracted from the vcf file with vcf2phylip (Ortiz, 2019) al-

lowing for a maximum of 50% missing data across each site. We concatenated all nuclear loci for a final alignment and analyzed the mitochondrial locus separately.

2.5. Phylogenetic reconstruction

2.5.1. Multi-species coalescent analyses of species-level relationships

Given the mixed support for some species-level relationships within the genus (Burgon et al., 2021; Rodríguez et al., 2017; Vences et al., 2014), we first employed a multi-species coalescent approach to infer the species tree for the six *Salamandra* species using one representative sample for every sub-species (23 samples total, Table S1). To verify that the result was not driven by increased sampling in certain species we additionally conducted the analyses with only one sample per species, choosing a sample most representative of the type-locality of the species (see Table S1). Due to the low average length of the loci in our dataset (average 351 bps), we did not pursue gene-tree based methods because poorly-supported gene trees are known to influence subsequent species-tree inference (Salichos and Rokas, 2013). Instead, we used a SNP based approach using SNAPP (Bryant et al., 2012), as implemented in Beast 2.6.0 (Bouckaert et al., 2014). SNAPP requires unlinked loci, thus we filtered the SNP dataset to only include one SNP per locus and not allowing for any missing data, resulting in a final dataset of 1,041 SNPs. The SNAPP input file was generated using BEAUti, calculating and sampling the mutation rates U and V from our data, and sampling the coalescence rate with a starting value of 10. Using the estimated age of the genus (Vences et al., 2014), we estimated a starting value for lambda (0.29) using the python script Pyule (available at https://github.com/joaks1/pyule) and applied a uniform distribution. Alpha and Beta for the theta prior were set to default, to explore a wide range of values. We ran SNAPP for 50 million generations, storing the chain every 1,000 trees and assessed convergence using Tracer v1.71 (Rambaut et al., 2018). Removing a burn-in of 10% of the trees, we depicted the remaining trees using DensiTree to visualize variation in the posterior distribution of topologies and branch lengths. A maximum clade credibility species tree was subsequently built using TreeAnnotator (Bouckaert et al., 2014) using the same burn-in of 10%.

2.5.2. Phylogenetic reconstruction of intraspecific relationships

As applying a multi-species coalescent approach to large datasets is computationally too demanding we used a concatenated approach for the dataset of 88 samples. We estimated the combined phylogeny and divergence times of our concatenated dataset of the two species with intraspecific variation in reproductive mode, *S. salamandra* (74 samples) and *S. algira* (14 samples), using Bayesian inference in BEAST 2.6.0 (Bouckaert et al., 2014) applying a relaxed molecular clock. We applied the coalescent bayesian skyline tree prior as our dataset was mostly population-based and only included two species (e.g. see Ritchie et al., 2017). The substitution model for the concatenated alignment was estimated during the BEAST run with bModelTest 1.1.0 (Bouckaert and Drummond, 2017). To time-calibrate the phylogeny we initially applied a prior for the split between *S. algira* and *S. salamandra* at 5.6 mya with a normal distribution and a sigma of 0.13. This corresponds to the estimated time of the Messinian Salinity Crisis which has been hypothesized to be responsible for the divergence of multiple amphibian species pairs across the strait of Gibraltar (Ehl et al., 2019). Applying this old prior to our concatenated dataset of population-level sampling caused a strong bias for older splits across the tree (see Fig S1), which is a known problem when applying Bayesian methods to concatenated alignments that likely include high levels of incomplete lineage sorting (ILS), discussed in numerous recent works (Mello et al., 2021; Stange et al., 2018; Tiley et al., 2020). To alleviate this issue, we added two recent priors for the estimated dates of the separation of the two continental island populations (Fig. 2B) based on both bathymetric (Dias et al., 2000) and genetic data (Lourenço et al., 2018b), by applying a normal distribution centered at 10.9 kya with a sigma of 0.004 to the node at the base of each clade of island samples. As adding recent priors in the presence of ILS can also shift older divergence dates (e.g. see Fang et al., 2020), we discuss the results of both analyses as an upper and lower bound to our divergence estimates. For each analysis we ran the MCMC chain twice for 100 million generations sampling every 5,000 generations and monitored convergence using Tracer v1.71 (Rambaut et al., 2018). We combined tree files using LogCombiner v1.8.4, removing the first 20% as burn-in and built a maximum clade credibility tree using TreeAnnotator (Bouckaert et al., 2014).

In addition to our Bayesian analyses, a maximum likelihood tree was estimated using RAxML 8.2.12 (Stamatakis, 2014) applying the GTRCAT substitution model on the concatenated nuclear alignment of all 94 samples and starting from ten parsimony informed trees and ten random trees. Bootstrap support was computed on the best scoring tree by means of 100 iterations of rapid bootstrapping (Stamatakis et al., 2008).

2.5.3. Mitochondrial barcoding of pregnant females

To determine the phylogenetic placement of all the pregnant females within the wider phylogeny of the sequence capture dataset, we used the CytB barcode. Sanger sequence chromatograms for 22 pregnant females were obtained and aligned using Geneious (Kearse et al., 2012). For the 94 sequence capture samples, we mapped all the filtered reads to the full *S. salamandra* mitochondrial genome (Mulder et al., 2016) using bowtie2 (Langmead and Salzberg, 2012) and kept only correctly paired reads. We inspected mapped reads for potential contamination and called consensus sequences requiring a minimum of 12 reads.

Complete sequences for both datasets were combined (N = 116), trimmed to 802 bps and aligned using MUSCLE 3.8.425 (Edgar, 2004) as implemented in Geneious prime 2019 (Kearse et al., 2012) for a maximum of eight iterations. We performed Bayesian phylogenetic analyses in BEAST version 2.6.1 (Drummond et al., 2012) on the CIPRES Science Gateway (Miller et al., 2010), and selected the optimal nucleotide substitution model (TrN) with JMODELTEST version 2.1.4 (Darriba et al., 2012), under the Bayesian information criterion (BIC). We performed three independent runs using an uncorrelated relaxed clock and a constant population size model as the coalescent tree prior, with a total of 100 million generations per run. We verified parameter convergence by examining the effective sample sizes (ESSs) in TRACER version 1.6 and removed the first 10% as burn-in. We obtained a maximum clade credibility summary tree with Bayesian posterior probabilities (BPP) for each node using TreeAnnotator v 1.8.4, and edited the resulting tree in Figtree version 1.4.3 (http://tree.bio.ed.ac.uk/software/figtree).

2.6. Ancestral state reconstruction of reproductive mode

To estimate the number of transitions between larviparity and pueriparity among lineages of *S. salamandra* and *S. algira*, we performed ancestral state reconstruction (ASR) on our two dated BEAST phylogenies (Fig. S1 and S2), coding the two reproductive modes as discrete characters. We based our character states on the results of the reproductive mode assessment in this study (Section 3.1) and previous work (Alarcón-Ríos et al., 2020b; Alarcón-ríos and Velo-antón, 2021; Buckley et al., 2007; Donaire-Barroso and Bogaerts, 2001; Galán, 2007; Niemiller et al., 2016; Uotila et al., 2013; Velo-Antón et al., 2015, 2007), identifying all *S. s. bernardezi*, *S. s. gallaica* from San Martiño and Ons, and *S. a. tingitana* from Northern Morocco as pueriparous (Fig. 2; Table S1 and S2). Although ASR is usually applied to phylogenies in which all tips are species, the approach can be applied to sub-specific level variation similar to that observed in the *Salamandra* system (Joy et al., 2016; Richmond, 2006). We performed stochastic character mapping using SIMMAP (Bollback, 2006) to estimate the ancestral reproductive modes across the phylogeny, and to estimate the number of in-

dependent transitions to pueriparity. We applied the make.simmap function in phytools 0.6 (Revell, 2012), as implemented in R 3.6.3 (R Core Team, 2020) on a random subset of 100 trees from the posterior distribution of the BEAST Bayesian inference after removal of the burn-in of 20% (Fig. S2). This method simulates character evolution along the phylogeny using an MCMC approach and samples the posterior distribution of transitions to estimate the probabilities of each character state on all nodes. We first used a likelihood-ratio test to compare the two different models of evolution (equal rates, and all-rates-different) between our two discrete characters, using the Akaike Information Criterion (AIC) to choose the best model. With the best-fit model (equal rates) we ran 10,000 MCMC simulations and mapped the posterior probabilities onto the phylogeny to identify the locations of putative reproductive mode transitions.

3. Results

3.1. Reproductive mode assessment

We confirmed pueriparity in all 35 *S. s. bernardezi* females. Clutch sizes were highly variable, with a mean clutch size of 8.9 individuals per female (range 1–24; Table S2). Together with fully metamorphosed juveniles, a few females delivered some gilled individuals, but in a very advanced stage of development. Those individuals had started the colouration change from typical greyish of larvae to black and yellow adult colouration and completed metamorphosis in a short period after parturition. The two *S. s. fastuosa* individuals were confirmed as larviparous as both females delivered fully aquatic larvae, with the typical greyish coloration and morphological traits of *S. salamandra* larvae and less variability in the stage of development within clutches compared to the pueriparous births.

3.2. Bioinformatic processing

Illumina NovaSeq S4 sequencing resulted in an average of 8.1 million paired-end reads per individual split between the 1,326 markers. After splitting the exons and manual filtering based on the initial SECAPR results on 12 individuals, our reference included 2,363 loci. Removing loci with excess heterozygosity and low coverage reduced this dataset to 2,287 loci (average coverage per individual 36, CI 5.6–78). Our 50% missing data threshold resulted in a total concatenated alignment of 574,577 bps.

3.3. Phylogenetic reconstruction

3.3.1. Multi-species coalescent tree for species level relationships

The DensiTree plot from the multi-species coalescent analyses (Fig. 3) revealed the uncertainty in the relationships among *S. atra, S. corsica* and *S. lanzai*; 66% of all topologies in the posterior distribution of phylogenies placed *S. corsica* and *S. lanzai* as sister species, whereas 9% placed *S. atra* and *S. lanzai* as sister species. The type locality analysis supported the same top two topologies with 34% and 31% of all trees respectively (Fig. S3). The consensus tree reflected this uncertainty with low support for these nodes. The posterior probability in the *S. salamandra, S. algira* node was low in the 23 individual analyses (0.85; Fig. 3), but high in the SNAPP analysis that only included the type localities (0.98; Fig. S3).

3.3.2. Dated phylogeny of the concatenated alignment

Bayesian inference with BEAST on the concatenated alignment of 88 samples, resolved the majority of nodes with high support (Fig. 4 and Fig. S1, S2, S6). The maximum likelihood tree largely followed the same general topology but node support was lower across some parts of the tree and the position of *S. lanzai* differed and had low support (Fig. S4). There were no differences in the nodes at the root of the four in-

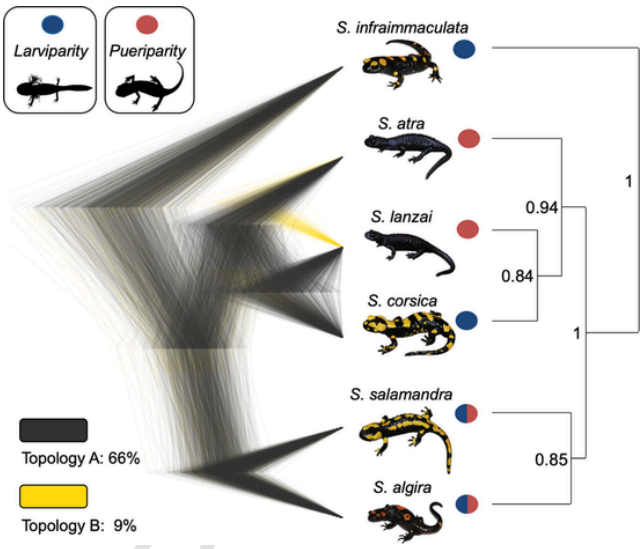

Fig. 3. DensiTree plot of 45,000 SNAPP trees of the 23 sub-species representing the 6 species in *Salamandra*. The most common topology is in dark grey (66%), and the second most common in yellow (9%). Remaining topologies have been removed for clarity. On the right is the consensus tree as generated by treeannotator and with posterior probabilities indicated on the nodes. (For interpretation of the references to color in this figure legend, the reader is referred to the web version of this article.)

traspecific transitions to pueriparity which were all strongly supported with a pp = 1 or a bootstrap score of > 99%.

Both species were monophyletic but some recognized subspecies formed paraphyletic groups. For instance, *S. s. gigliolii* sits within the *S. s. fastuosa* clade, which in turn is sister to the *S. s. bernardezi* clade, supporting recent findings for *S. salamandra* subspecies relationships (Burgon et al., 2021). Likewise, several individuals that were identified as *S. s. bejarae* based on locality and morphology are within the larger *S. s. gallaica* clade, whereas *S. s. bejarae* from the locality Candelario, ~3 km away from the type locality (Bejar), were placed outside of the S. *s. gallaica* clade in a monophyletic lineage (Fig. S1 and S2).

3.3.3. Mitochondrial barcoding of pregnant females

We obtained CytB barcode sequences for 22 pregnant females across the *S. s. bernardezi* (N = 25) and *S. s. fastuosa* (N = 1) range (see Table S2). They were placed in the *S. s. bernardezi* mtDNA clade and included representatives of all major lineages within the subspecies, with the exception of two *S. s. bernardezi* samples and the single *S. s. fastuosa* sample, which were identified as *S. s. gallaica* mtDNA (Fig. S5). All of them show phenotypic characters typical of *S. s. bernardezi-fastuosa* (striped coloration pattern, round snout shape and small body size; Alarcón-Ríos et al., 2020a), consistent with previous reports of mitochondrial introgression across the *S. s. bernardezi* range (Figueiredo-Vázquez et al., 2021; Lourenço et al., 2019; Velo-Antón et al., 2021).

3.4. Ancestral state reconstruction reveals five independent transitions to pueriparity

The equal rates transition rate model was the best fit to our dataset and the Bayesian inference ancestral state reconstruction indicated a total of four independent transitions to pueriparity (Fig. 4) with no reversals to larviparity. There was additionally at least one transition to pueriparity for *S. atra/S. lanzai* based on the multi-species coalescent analyses. The intraspecific transitions included two independent transitions on the continental islands of Ons and San Martiño in the late Pleistocene or Holocene, one in the northern populations of *S. a tingitana* that likely occurred during the late Pleistocene and one transition in the subspecies *S. s. bernardezi* that occurred in the early to mid Pleistocene.

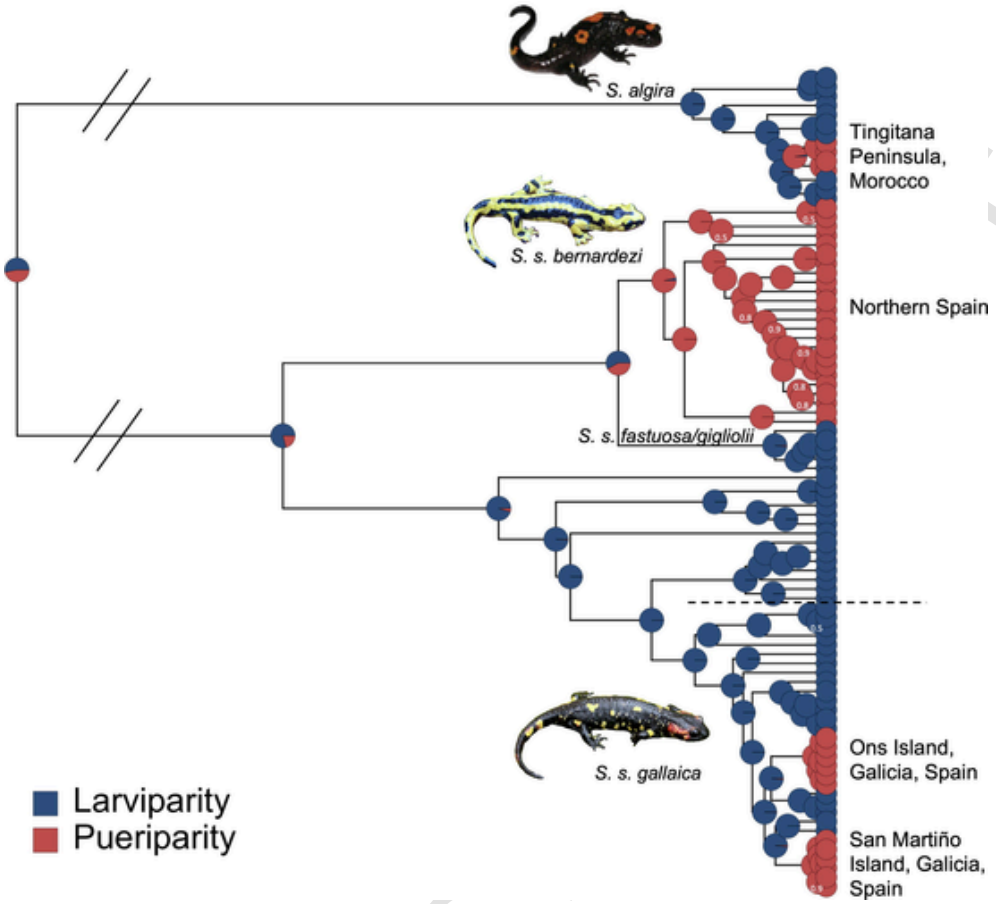

Fig. 4. Bayesian inference based on a concatenated dataset of 574 k bps of 88 samples of *S. salamandra* and *S. algira*. The tips of the tree are coded by reproductive mode, blue for larviparity and red for the pueriparity. Node support under 1.0 indicated in white. The results of the ancestral state reconstruction are placed on the internal nodes. Sub-species designation and location are included in Fig. S2. Samples corresponding to the *S. s. gallaica* clade are indicated by the dashed line. (For interpretation of the references to color in this figure legend, the reader is referred to the web version of this article.)

The results of the ancestral state reconstruction on the second beast phylogeny (Fig. S1), were very similar with the same transitions found across the tree (Fig. S6).

4. Discussion

Our study provides strong support for a minimum of five independent transitions to pueriparity across multiple timescales in the genus *Salamandra*, indicating that different combinations of climatic and local evolutionary pressures may lead to the development of this complex trait. In addition, we demonstrate that sequence capture using transcriptome-based loci can produce high quality data to estimate phylogenetic relationships at both inter- and intraspecific levels, even for the large genomes of urodeles (Gregory, 2003; Weisrock et al., 2018). Finally, our increased geographic sampling of documented births and their phylogenetic position confirms that *S. s. bernardezi* is pueriparous across its geographic range and all phylogenetic sub-lineages, and can be considered fully pueriparous.

4.1. Systematic revision within Salamandra salamandra

Many subspecies have been described for *Salamandra salamandra*, but some lack genetic support for these designations (see Burgon et al., 2021). Our phylogenetic analyses confirm that two Iberian subspecies require systematic revision. *Salamandra s. bejarae* is considered to have a wide range across much of central Iberia (Fig. 1), but the majority of our samples from that area grouped within the larger *S. s. gallaica* clade. This supports previous results revealing *S. s. bejarae* as paraphyletic to *S. s. gallaica* across the mountains of the Iberian Central System (Antunes et al., 2021; Pereira et al., 2016). Given that one *S. s. bejarae* sample (Candelario), representative of the type locality (Béjar), was distinct from *S. s. gallaica* and the other samples across the assumed *S. s. bejarae* range, it is possible that *S. s. bejarae* is indeed monophyletic, but inhabits a much smaller geographic area than is presently attributed to the subspecies. Likewise, *S. s. gigliolii* occurs entirely within the larger clade of *S. s. fastuosa* from northern Iberia suggesting that its current allopatric distribution in Italy is the result of a past range expansion from an ancestral *S. s. fastuosa* population (Burgon et al., 2021).

4.2. Complex evolutionary history of S. atra/lanzai/corsica clade, and uncertainty in the number of transitions to pueriparity

The topology with the highest support as found by multi-species coalescent analyses in SNAPP included *S. lanzai* and *S. corsica* as sister species, and *S. atra* as sister to this clade. However, a substantial part of the posterior distribution also supported a monophyletic grouping of the two pueriparous species (*S. atra* and *S. lanzai*), corroborating previous studies based on a RNAseq and ddRAD data of the genus (Burgon et al., 2021; Rodríguez et al., 2017). This would also be the most parsimonious explanation when considering that both alpine species are geographically close, compared to the insular *S. s. corsica*, and that they are melanistic and pueriparous. Pueriparity in both species also includes multiple comparable adaptations like long-pregnancy times, and reduced offspring number that make a single transition to pueriparity more likely.

The complicated history of *S. corsica*, *S. atra* and *S. lanzai* could be explained by introgression, and at least one instance of introgression is suspected from the mitochondrial gene tree which shows a different topology than the multi-species coalescent-based estimates with nuclear data (Fig. S5, and Fig. 4 in Rodríguez et al. 2017). This complicated history has been hypothesized to be caused by the Messinian Salinity Crisis (5.6 mya, Pliocene) during which the desiccation of the Mediterranean Sea may have resulted in the simultaneous isolation and speciation in this clade of three species. This created short inter-nodes, which can be difficult to resolve even with large amounts of data (Salichos and Rokas, 2013). This hypothesis would suggest that mitochondrial introgression also occurred early in the history of the three species as they have likely been parapatric since then (Burgon et al., 2021; Rodríguez et al., 2017; Vences et al., 2014). Interestingly, the sister species *S. salamandra* and *S. algira*, which also diverged at the end of Messinian Salinity Crisis (Vences et al., 2014), are well differentiated at both mtDNA or nuDNA levels, with little signs of introgression. Given the high uncertainty in this node across multiple datasets and analyses, we cannot distinguish between a single transition for both *S. atra* and *S. lanzai*, the possibility of two independent transitions to pueriparity, or that the common ancestor to all three species was pueriparous and that there was a subsequent reversal to larviparity in *S. corsica*.

4.3. A Pleistocene transition in S. s. bernardezi and retained larviparity for the sister clade of S. s. fastuosa and S. s. gigliolii

Salamandra s. bernardezi is considered to be a pueriparous subspecies, but its parity had only been confirmed from a few localities (see Table S2). Our direct observations of births at 20 localities across the subspecies range including several distinct genetic lineages (Fig. 2A & Fig. S5), confirm that pueriparity is likely the prevailing parity mode for this subspecies. In our phylogenetic analyses, *S. s. bernardezi* is sister to the combined clade of *S. s. fastuosa* (both larviparity and pueriparity documented) and *S. s. gigliolii* (only larviparity documented). Although there are confirmations of pueriparity in some *S. s. fastuosa* individuals, it does not appear to be the prevailing mode in this subspecies (see Uotila et al., 2013; presence of larvae across the entire *S. s. fastuosa* range, GVA observations). The original hypothesis by García-París et al. (2003) suggests that instances of pueriparity, and bernardezi-like color pattern and head shape in *S. s. fastuosa* are due to introgression from *S. s. bernardezi* into *S. s. fastuosa* via male biased dispersal. Mito-nuclear discordances in *S. salamandra* are quite common and have been attributed to male biased dispersal (Antunes et al., 2021; Bisconti et al., 2018; García-París et al., 2003; Velo-Antón et al., 2021) and high philopatry in females (Helfer et al., 2012; Lourenço et al., 2018a). The proposed topology and demographic history would correspond with a single transition to pueriparity in *S. s. bernardezi* in the Pleistocene (0.26–1.78 mya), retained larviparity in *S. s. fastuosa* and *S. s. gigliolii*, and subsequent introgression of pueriparity into *S. s. fastuosa*. More direct observations of parity mode across the range of *S. s. fastuosa* coupled with nuclear genetic data and demographic modeling are needed to fully explore and test these hypotheses.

4.4. A late Pleistocene transition in S. algira followed by mitochondrial introgression

To date there are few scientifically documented pueriparous births in *S. algira* (Dinis and Velo-Antón, 2017; Donaire-Barroso et al., 2001; Donaire-Barroso and Bogaerts, 2001). Most pueriparous populations fall within a single mtDNA sublineage of *S. a. tingitana*, which occurs across the northern Tingitana Peninsula in Morocco (north of the river Oued Martil; Dinis et al., 2019), where the scarce water bodies lack salamander larvae. However, pueriparity was also confirmed in one neighboring population, south of this river, which belongs to a distinct mtDNA sublineage of *S. a. tingitana*, and suggests another case of mtDNA introgression between sister taxa across a contact zone (Dinis and Velo-Antón, 2017). The nuclear phylogeny shows that all the pueriparous populations (Fig. 2C) form one clade, which suggests a single transition to pueriparity in the late Pleistocene (37–473kya). All confirmed pueriparous populations are found in areas with little to no surface water, low average precipitation in the coldest quarter, and populations retreating to karstic systems during dry periods (Beukema et al., 2010). Correspondingly, the geographic extent of this single nuclear clade overlaps strongly with the predicted distribution of pueriparity based on environmental models (Beukema et al., 2010). This predicted distribution combined with our nuclear and mitochondrial data suggests that pueriparity evolved once above the Oued (river) Martil and likely expanded south via male biased dispersal to Amsa and Tetouan into this suitable pueriparous habitat (Fig. 2C).

4.5. Two independent transitions in S. s. gallaica on the continental islands of Ons and San Martiño

The insular populations of San Martiño and Ons are both pueriparous (Alarcón-Ríos et al., 2020b; Velo-Antón et al., 2015, 2012, 2007) but their phylogenetic relationships to the mainland were still unclear in previous studies. Our strongly supported topology indicates that the San Martiño and Ons populations are not each other's closest relatives and that they independently became separated from their closest mainland populations. The Ons population is closely related to the larviparous population on the Grove peninsula (a former island reconnected to the mainland with the deposition of river sediments during the XVII-XVIII centuries; see Velo-Antón et al., 2012), which is consistent with bathymetric data that connect those corresponding regions at lower sea levels (Fig. 2B; Lourenço et al., 2018b). San Martiño is closely related to the Monteferro peninsula, which is its geographically closest mainland population but which shows a deeper bathymetric depression compared to the Morrazo peninsula (e.g. Melide and Nerga populations). Correspondingly, the ASR supports two independent transitions to pueriparity from the ancestral larviparous state in *S. s. gallaica*. The estimated divergence dates for the island lineages varied widely due to influence of ILS on our two approaches to divergence dating (Ons: 20.4–727 kya and San Martiño 21.4–659 kya). The islands were formed during the sea level rise after the last glacial maximum during the early Holocene (ca. 8–6 kya; Dias et al., 2000), which is assumed to be the biogeographic event that isolated the present insular populations from the mainland counterparts (Lourenço et al., 2018b; Velo-Antón et al., 2007; 2012). Overestimation of recent node ages is a known bias in divergence dating approaches, especially when using population level genetic data (Ho et al., 2005), skewed dating priors (Duchêne et al., 2014; Phillips, 2009), and under high levels of ILS (Fang et al., 2020). Thus, although our molecular divergence date estimates span a wide time interval, the Holocene formation of the islands and subsequent appearance of pueriparity appears the most likely scenario. On the other hand, the presence of individuals with mixed reproductive mode in Monteferro where some females of this predominantly larviparous population laid both fully metamorphosed juveniles and young larvae or larvae at a later developmental stage (Velo-Antón et al., 2015) may indicate that pueriparity evolved earlier than the formation of the islands. However, this scenario would likely imply more divergent mitochondrial haplotypes (as occurs in *S. s. tingitana*), while there is mtDNA haplotype sharing occurs across populations of this island-mainland system (Lourenço et al., 2018b; Velo-Antón et al., 2012, 2007). Thus, whether females delivering mixed offspring is a retention of a previous pueriparous ancestral state or the result of an ongoing adaptive process to pueriparity is still unknown and will require analyses that correct for the influence of ILS and that include additional independent dating priors.

4.6. Conclusion

Our analyses indicate that the transition to pueriparity has occurred at least five times in the genus *Salamandra*. Transitions to pueriparity arose at different evolutionary time periods ranging from the Pliocene to the late Pleistocene or Holocene, suggesting that a combination of climatic and local environmental conditions form the evolutionary pressures that lead to this major life-history transition. The number of transitions between reproductive mode is remarkable considering the age of the clade and the number of species. Intraspecific variation in reproductive mode is also rare, and to our knowledge this is the only case in which this occurs in two sister-species. The putative introgression events at multiple phylogenetic levels, as evident from the numerous cases of mito-nuclear discordance, also highlights the potential that reproductive mode shifts can lead to adaptive geographic expansions along suitable habitat. Combining this phylogenetic framework with environmental data can help us understand the evolutionary pressures that contribute to shifts in reproductive mode.

Much of the research on viviparity has focused on squamates given the high number of transitions across this large clade (Blackburn, 2015). We propose that the genus *Salamandra* and its pueriparous sister clade *Lyciasalamandra* are an excellent parallel case-study to investigate both the transition to viviparity, and the distinction between larviparity and pueriparity. In particular, convergent evolution of pueriparity at multiple timescales is ideal for further research into the adaptive genomic architecture of this complex trait and the evolutionary and ecological context in which it is adaptive.

Declaration of Competing Interest

The authors declare that they have no known competing financial interests or personal relationships that could have appeared to influence the work reported in this paper.

Acknowledgements

We thank Nancy McInerney and Jeff Hunt for facilitating lab work at the Center for Conservation Genomics and the Laboratory of Analytical Biology respectively. Brian Brunelle and Alison Devault at Arbor Biosciences for help and advice on bait design. Lillian Parker was instrumental in developing and optimizing the library prep protocol. Thanks to Duarte Gonçalves and Ivan Prates for their insights on the analyses, Robert Wilson and Addison Wynn for logistical support and André Lourenço, Marco Dinis and Adam Marques for assistance in the lab. Miguel Vences, Sebastian Steinfartz, Nikolay Tzankov, Pim Arntzen, Wouter Beukema, André Lourenço, Helena Gonçalvez, Luis García Cardenete, Antigoni Kalionzopoulou and Fernando Martínez-Freiría for providing tissue samples from some *Salamandra* lineages or help during field work, and Miguel Vences for pictures of several of the species and feedback on an earlier draft of the manuscript. We thank two anonymous reviewers and the editor for constructive feedback on an earlier version of this manuscript. Portions of the laboratory and computer work were conducted in and with the support of the L.A.B. facilities of the National Museum of Natural History (NMNH). The computations performed for this paper were conducted on the Smithsonian High Performance Cluster (SI/HPC), Smithsonian Institution. https://doi.org/10.25572/SIHPC. Financial support came from National Funds through FCT – Foundation for Science and Technology (SALOMICS: PTDC/BIA-EVL/28475/2017); the authors also acknowledge funding from other FCT projects and FEDER funds through the Operational Programme for Competitiveness Factors – COMPETE (EVOVIV: PTDC/BIA- EVF/3036/2012; FCOMP-01-0124-FEDER-028325 and UIDB/500027/2020); and by the office of the Associate Director of Science at the Smithsonian's National Museum of Natural History. KPM was funded by an FCT predoctoral grant (PD/BD/52604/2014) and GVA by FCT research contracts (IF/01425/2014 and CEECIND/00937/2018), all from the Portuguese "Fundacão para a Ciência e a Tecnologia," funded by Programa Operacional Potencial Humano (POPH)-Quadro de Referência Estratégica Nacional (QREN) from the European Social Fund.

Appendix A. Supplementary material

Supplementary data to this article can be found online at https://doi.org/10.1016/j.ympev.2021.107347.

References

Alarcón-ríos, L., Velo-antón, G., 2021. Short Note Multiple paternity in the pueriparous North African fire salamander , Salamandra algira , supports polyandry as a successful mating strategy in low fecundity Salamandra lineages. https://doi.org/10.1163/15685381-bja10075

Alarcón-Ríos, L., Nicieza, A.G., Kaliontzopoulou, A., Buckley, D., Velo-Antón, G., 2020a. Evolutionary history and not heterochronic modifications associated with viviparity drive head shape differentiation in a reproductive polymorphic species, Salamandra salamandra. Evol. Biol. 47, 43–55. https://doi.org/10.1007/s11692-019-09489-3

Alarcón-Ríos, L., Nicieza, A.G., Lourenço, A., Velo-Antón, G., 2020b. The evolution of pueriparity maintains multiple paternity in a polymorphic viviparous salamander. Sci. Rep. 10, 1–8. https://doi.org/10.1038/s41598-020-71609-3

Andermann, T., Cano, Á., Zizka, A., Bacon, C., Antonelli, A., 2018. SECAPR - A bioinformatics pipeline for the rapid and user-friendly processing of targeted enriched Illumina sequences, from raw reads to alignments. PeerJ 2018, e5175. https://doi.org/10.7717/peerj.5175

Antunes, B., Velo-Antón, G., Buckley, D., Pereira, R.J., Martínez-Solano, I., 2021. Physical and ecological isolation contribute to maintain genetic differentiation between fire salamander subspecies. Heredity (Edinb). 126 (5), 776–789. https://doi.org/10.1038/s41437-021-00405-0.

Beukema, W., De Pous, P., Donaire, D., Escoriza, D., Bogaerts, S., Toxopeus, A.G., De Bie, C.A.J.M., Roca, J., Carranza, S., 2010. Biogeography and contemporary climatic differentiation among Moroccan Salamandra algira. Biol. J. Linn. Soc. 101, 626–641. https://doi.org/10.1111/j.1095-8312.2010.01506.x.

Beukema, W., Nicieza, A.G., Lourenço, A., Velo-Antón, G., 2016. Colour polymorphism in *Salamandra salamandra* (Amphibia: Urodela), revealed by a lack of genetic and environmental differentiation between distinct phenotypes. J. Zool. Syst. Evol. Res. 54, 127–136. https://doi.org/10.1111/jzs.12119.

Birol, I., Jackman, S.D., Nielsen, C.B., Qian, J.Q., Varhol, R., Stazyk, G., Morin, R.D., Zhao, Y., Hirst, M., Schein, J.E., Horsman, D.E., Connors, J.M., Gascoyne, R.D., Marra, M.A., Jones, S.J.M., 2009. De novo transcriptome assembly with ABySS. Bioinformatics 25 (21), 2872–2877. https://doi.org/10.1093/bioinformatics/btp367.

Bisconti, R., Porretta, D., Arduino, P., Nascetti, G., Canestrelli, D., 2018. Hybridization and extensive mitochondrial introgression among fire salamanders in peninsular Italy. Sci. Rep. 8, 1–10. https://doi.org/10.1038/s41598-018-31535-x.

Blackburn, D.G., 2015. Evolution of vertebrate viviparity and specializations for fetal nutrition: A quantitative and qualitative analysis. J. Morphol. 276 (8), 961–990. https://doi.org/10.1002/jmor.v276.810.1002/jmor.20272.

Bollback, J.P., 2006. SIMMAP: Stochastic character mapping of discrete traits on phylogenies. BMC Bioinform. 7, 1–7. https://doi.org/10.1186/1471-2105-7-88.

Bouckaert, R.R., Drummond, A.J., 2017. bModelTest: Bayesian phylogenetic site model averaging and model comparison. BMC Evol. Biol. 17, 1–11. https://doi.org/10.1186/s12862-017-0890-6.

Bouckaert, R.R., Heled, J., Kühnert, D., Vaughan, T., Wu, C.H., Xie, D., Suchard, M.A., Rambaut, A., Drummond, A.J., 2014. BEAST 2: A Software Platform for Bayesian Evolutionary Analysis. PLoS Comput. Biol. 10, 1–6. https://doi.org/10.1371/journal.pcbi.1003537

Bryant, D., Bouckaert, R.R., Felsenstein, J., Rosenberg, N.A., Roychoudhury, A., 2012. Inferring species trees directly from biallelic genetic markers: Bypassing gene trees in a full coalescent analysis. Mol. Biol. Evol. 29, 1917–1932. https://doi.org/10.1093/molbev/mss086.

Buckley, D., 2012. Evolution of Viviparity in Salamanders (Amphibia, Caudata). eLS. https://doi.org/10.1002/9780470015902.a0022851

Buckley, D., Alcobendas, M., García-París, M., Wake, M.H., 2007. Heterochrony, cannibalism, and the evolution of viviparity in Salamandra salamandra. Evol. Dev. 9, 105–115. https://doi.org/10.1111/j.1525-142X.2006.00141.x.

Burgon, J.D., Vences, M., Steinfartz, S., Bogaerts, S., Bonato, L., Donaire-Barroso, D., Martínez-Solano, I., Velo-Antón, G., Vieites, D.R., Mable, B.K., Elmer, K.R., 2021. Phylogenomic inference of species and subspecies diversity in the Palearctic salamander genus Salamandra. Mol. Phylogenet. Evol. 157, 107063. https://doi.org/10.1016/j.ympev.2020.107063.

Carøe, C., Gopalakrishnan, S., Vinner, L., Mak, S.S.T., Sinding, M.H.S., Samaniego, J.A., Wales, N., Sicheritz-Pontén, T., Gilbert, M.T.P., 2018. Single-tube library preparation for degraded DNA. Methods Ecol. Evol. 9, 410–419. https://doi.org/10.1111/2041-210X.12871.

Darriba, D., Taboada, G.L., Doallo, R., Posada, D., 2012. jModelTest 2: more models, new heuristics and parallel computing. Nat. Methods 9 (8), 772. https://doi.org/10.1038/nmeth.2109.

Deleury, E., Guillemaud, T., Blin, A., Lombaert, E., 2019. An evaluation of pool-

sequencing transcriptome-based exon capture for population genomics in non-model species. bioRxiv 583534. https://doi.org/10.1101/583534
Dias, J.M.A., Boski, T., Rodrigues, A., Magalhães, F., 2000. Coast line evolution in Portugal since the Last Glacial Maximum until present - A synthesis. Mar. Geol. 170 (1–2), 177–186. https://doi.org/10.1016/S0025-3227(00)00073-6.
Dinis, M., Merabet, K., Martínez-Freiría, F., Steinfartz, S., Vences, M., Burgon, J.D., Elmer, K.R., Donaire, D., Hinckley, A., Fahd, S., Joger, U., Fawzi, A., Slimani, T., Velo-Antón, G., 2019. Allopatric diversification and evolutionary melting pot in a North African Palearctic relict: The biogeographic history of Salamandra algira. Mol. Phylogenet. Evol. 130, 81–91. https://doi.org/10.1016/j.ympev.2018.10.018.
Dinis, M., Velo-Antón, G., 2017. How little do we know about the reproductive mode in the North African salamander, Salamandra algira? Pueriparity in divergent mitochondrial lineages of S. a. tingitana. Amphibia-Reptilia 38, 540–546. https://doi.org/10.1163/15685381-00003121.
Donaire-Barroso, D., Bogaerts, S., 2001. Observations on viviparity of Salamandra algira in North Morocco. Herpetol. Candiana 147–151.
Donaire-Barroso, D., Bogaerts, S., Herbert, D., 2001. Confirmación de desarrollo larvario completo intrauterino en Salamandra algira (Bedriaga, 1883) del noroeste de Marruecos. Butll. la Soc. Catalana d'Herpetologia 15, 107–110.
Drummond, A.J., Suchard, M.A., Xie, D., Rambaut, A., 2012. Bayesian phylogenetics with BEAUti and the BEAST 1.7. Mol. Biol. Evol. 29, 1969–1973. https://doi.org/10.1093/molbev/mss075.
Duchêne, S., Lanfear, R., Ho, S.Y.W., 2014. The impact of calibration and clock-model choice on molecular estimates of divergence times. Mol. Phylogenet. Evol. 78, 277–289. https://doi.org/10.1016/j.ympev.2014.05.032.
Edgar, R.C., 2004. MUSCLE: Multiple sequence alignment with high accuracy and high throughput. Nucleic Acids Res. 32 (5), 1792–1797. https://doi.org/10.1093/nar/gkh340.
Ehl, S., Vences, M., Veith, M., 2019. Reconstructing evolution at the community level: A case study on Mediterranean amphibians. Mol. Phylogenet. Evol. 134, 211–225. https://doi.org/10.1016/j.ympev.2019.02.013.
Fang, B., Merilä, J., Matschiner, M., Momigliano, P., 2020. Estimating uncertainty in divergence times among three-spined stickleback clades using the multispecies coalescent. Mol. Phylogenet. Evol. 142, 106646. https://doi.org/10.1016/j.ympev.2019.106646.
Figueiredo-Vázquez, C., Lourenço, A., Velo-Antón, G., 2021. Riverine barriers to gene flow in a salamander with both aquatic and terrestrial reproduction. Evol. Ecol. 35 (3), 483–511. https://doi.org/10.1007/s10682-021-10114-z.
Frost, D.R., 2021. Amphibian Species of the World: an Online Reference. Version 6.1. American Museum of Natural History [WWW Document]. URL research.amnh.org/vz/herpetology/amphibia (accessed 5.16.20).
Galán, P., 2007. Viviparismo y distribución de Salamandra salamandra bernardezi en el norte de Galicia. Boletín la Asoc. Herpetológica Española 44–48.
García-París, M., Alcobendas, M., Buckley, D., Wake, D.B., 2003. Dispersal of viviparity across contact zones in Iberian populations of fire salamanders (Salamandra) inferred from discordance of genetic and morphological traits. Evolution (N. Y). 57, 129–143. https://doi.org/10.1111/j.0014-3820.2003.tb00221.x
Gower, D.J., Giri, V., Dharne, M.S., Shouche, Y.S., 2008. Frequency of independent origins of viviparity among caecilians (Gymnophiona): Evidence from the first "live-bearing" Asian amphibian. J. Evol. Biol. 21, 1220–1226. https://doi.org/10.1111/j.1420-9101.2008.01577.x.
Gregory, T.R., 2003. Variation across amphibian species in the size of the nuclear genome supports a pluralistic, hierarchical approach to the C-value enigma. Biol. J. Linn. Soc. 79, 329–339. https://doi.org/10.1046/j.1095-8312.2003.00191.x.
Greven, H., 2003. Larviparity and pueriparity, in: Reproductive Biology and Phylogeny of Urodela. CRC Press, pp. 447–475.
Harris, R.S., 2007. Improved pairwise Alignment of genomic DNA. Pennsylvania State University.
Helfer, V., Broquet, T., Fumagalli, L., 2012. Sex-specific estimates of dispersal show female philopatry and male dispersal in a promiscuous amphibian, the alpine salamander (Salamandra atra). Mol. Ecol. 21 (19), 4706–4720. https://doi.org/10.1111/j.1365-294X.2012.05742.x.
Helmstetter, A.J., Papadopulos, A.S.T., Igea, J., Van Dooren, T.J.M., Leroi, A.M., Savolainen, V., 2016. Viviparity stimulates diversification in an order of fish. Nat. Commun. 7, 1–7. https://doi.org/10.1038/ncomms11271.
Ho, S.Y.W., Phillips, M.J., Cooper, A., Drummond, A.J., 2005. Time dependency of molecular rate estimates and systematic overestimation of recent divergence times. Mol. Biol. Evol. 22, 1561–1568. https://doi.org/10.1093/molbev/msi145.
Iskandar, D.T., Evans, B.J., McGuire, J.A., 2014. A novel reproductive mode in frogs: A new species of fanged frog with internal fertilization and birth of tadpoles. PLoS One 9, 1–14. https://doi.org/10.1371/journal.pone.0115884
Joy, J.B., Liang, R.H., McCloskey, R.M., Nguyen, T., Poon, A.F.Y., 2016. Ancestral Reconstruction. PLoS Comput. Biol. 12, 1–20. https://doi.org/10.1371/journal.pcbi.1004763
Kearse, M., Moir, R., Wilson, A., Stones-Havas, S., Cheung, M., Sturrock, S., Buxton, S., Cooper, A., Markowitz, S., Duran, C., Thierer, T., Ashton, B., Meintjes, P., Drummond, A., 2012. Geneious Basic: An integrated and extendable desktop software platform for the organization and analysis of sequence data. Bioinformatics 28 (12), 1647–1649. https://doi.org/10.1093/bioinformatics/bts199.
Kircher, M., Sawyer, S., Meyer, M., 2012. Double indexing overcomes inaccuracies in multiplex sequencing on the Illumina platform. Nucleic Acids Res. 40, 1–8. https://doi.org/10.1093/nar/gkr771.
Langmead, B., Salzberg, S.L., 2012. Fast gapped-read alignment with Bowtie 2. Nat. Methods 9 (4), 357–359. https://doi.org/10.1038/nmeth.1923.
Li, H., Durbin, R., 2009. Fast and accurate short read alignment with Burrows-Wheeler transform. Bioinformatics 25 (14), 1754–1760. https://doi.org/10.1093/bioinformatics/btp324.
Liedtke, H.C., Müller, H., Hafner, J., Penner, J., Gower, D.J., Mazuch, T., Rödel, M.-O., Loader, S.P., 2017. Terrestrial reproduction as an adaptation to steep terrain in African toads. Proc. R. Soc. B Biol. Sci. 284 (1851), 20162598. https://doi.org/10.1098/rspb.2016.2598.
Lourenço, A., Antunes, B., Wang, I.J., Velo-Antón, G., 2018a. Fine-scale genetic structure in a salamander with two reproductive modes: Does reproductive mode affect dispersal? Evol. Ecol. 32 (6), 699–732. https://doi.org/10.1007/s10682-018-9957-0.
Lourenço, A., Gonçalves, J., Carvalho, F., Wang, I.J., Velo-Antón, G., 2019. Comparative landscape genetics reveals the evolution of viviparity reduces genetic connectivity in fire salamanders. Mol. Ecol. 28 (20), 4573–4591. https://doi.org/10.1111/mec.v28.2010.1111/mec.15249.
Lourenço, A., Sequeira, F., Buckley, D., Velo-Antón, G., 2018b. Role of colonization history and species-specific traits on contemporary genetic variation of two salamander species in a Holocene island-mainland system. J. Biogeogr. 45 (5), 1054–1066. https://doi.org/10.1111/jbi.2018.45.issue-510.1111/jbi.13192.
McKenna, A., Hanna, M., Banks, E., Sivachenko, A., Cibulskis, K., Kernytsky, A., Garimella, K., Altshuler, D., Gabriel, S., Daly, M., DePristo, M.A., 2010. The genome analysis toolkit: A MapReduce framework for analyzing next-generation DNA sequencing data. Genome Res. 20 (9), 1297–1303. https://doi.org/10.1101/gr.107524.110.
Mello, B., Tao, Q., Barba-Montoya, J., Kumar, S., 2021. Molecular dating for phylogenies containing a mix of populations and species by using Bayesian and RelTime approaches. Mol. Ecol. Resour. 21 (1), 122–136. https://doi.org/10.1111/men.v21.110.1111/1755-0998.13249.
Miller, M.A., Pfeiffer, W., Schwartz, T., 2010. Creating the CIPRES Science Gateway for inference of large phylogenetic trees. 2010 Gatew. Comput. Environ. Work. GCE 2010. https://doi.org/10.1109/GCE.2010.5676129
Mulder, K.P., Lourenço, A., Carneiro, M., Velo-Antón, G., 2016. The complete mitochondrial genome of Salamandra salamandra (Amphibia: Urodela: Salamandridae). Mitochondrial DNA Part B Resour. 1 (1), 880–882. https://doi.org/10.1080/23802359.2016.1253042.
Niemiller, M.L., Glorioso, B.M., Fenolio, D.B., Reynolds, R.G., Taylor, S.J., Miller, B.T., 2016. Growth, Survival, Longevity, and Population Size of the Big Mouth Cave Salamander (Gyrinophilus palleucus necturoides) from the Type Locality in Grundy County, Tennessee, USA. Copeia 104 (1), 35–41. https://doi.org/10.1643/OT-14-197.
Ortiz, E.M., 2019. vcf2phylip v2. 0: convert a VCF matrix into several matrix formats for phylogenetic analysis. Version v2.
Pereira, R.J., Martínez-Solano, I., Buckley, D., 2016. Hybridization during altitudinal range shifts: Nuclear introgression leads to extensive cyto-nuclear discordance in the fire salamander. Mol. Ecol. 25 (7), 1551–1565. https://doi.org/10.1111/mec.13575.
Phillips, M.J., 2009. Branch-length estimation bias misleads molecular dating for a vertebrate mitochondrial phylogeny. Gene 441 (1–2), 132–140. https://doi.org/10.1016/j.gene.2008.08.017.
Pincheira-Donoso, D., Tregenza, T., Witt, M.J., Hodgson, D.J., 2013. The evolution of viviparity opens opportunities for lizard radiation but drives it into a climatic cul-de-sac. Glob. Ecol. Biogeogr. 22 (7), 857–867. https://doi.org/10.1111/geb.12052.
R Core Team, 2020. R: A Language and Environment for Statistical Computing.
Rambaut, A., Drummond, A.J., Xie, D., Baele, G., Suchard, M.A., 2018. Posterior summarization in Bayesian phylogenetics using Tracer 1.7. Syst. Biol. 67, 901–904. https://doi.org/10.1093/sysbio/syy032
Recknagel, H., Kamenos, N.A., Elmer, K.R., 2021. Evolutionary origins of viviparity consistent with palaeoclimate and lineage diversification. J. Evol. Biol. 34, 1167–1176. https://doi.org/10.1111/jeb.13886
Revell, L.J., 2012. phytools: An R package for phylogenetic comparative biology (and other things). Methods Ecol. Evol. 3, 217–223. https://doi.org/10.1111/j.2041-210X.2011.00169.x
Reynolds, J.D., Goodwin, N.B., Freckleton, R.P., 2002. Evolutionary transitions in parental care and live bearing in vertebrates. Philos. Trans. R. Soc. B Biol. Sci. 357, 269–281. https://doi.org/10.1098/rstb.2001.0930
Richmond, J.Q., 2006. Evolutionary basis of parallelism in North American scincid lizards. Evol. Dev. 8, 477–490. https://doi.org/10.1111/j.1525-142X.2006.00121.x
Ritchie, A.M., Lo, N., Ho, S.Y.W., 2017. The impact of the tree prior on molecular dating of data sets containing a mixture of inter- and intraspecies sampling. Syst. Biol. 66, 413–425. https://doi.org/10.1093/sysbio/syw095
Rodríguez, A., Burgon, J.D., Lyra, M., Irisarri, I., Baurain, D., Blaustein, L., Göçmen, B., Künzel, S., Mable, B.K., Nolte, A.W., Veith, M., Steinfartz, S., Elmer, K.R., Philippe, H., Vences, M., 2017. Inferring the shallow phylogeny of true salamanders (Salamandra) by multiple phylogenomic approaches. Mol. Phylogenet. Evol. 115, 16–26. https://doi.org/10.1016/j.ympev.2017.07.009.
Salichos, L., Rokas, A., 2013. Inferring ancient divergences requires genes with strong phylogenetic signals. Nature 497 (7449), 327–331. https://doi.org/10.1038/nature12130.
Sandberger-Loua, L., Müller, H., Rödel, M.O., 2017. A review of the reproductive biology of the only known matrotrophic viviparous anuran, the West African Nimba toad, Nimbaphrynoides occidentalis. Zoosystematics Evol. 93, 105–133. https://doi.org/10.3897/ZSE.93.10489
Stamatakis, A., 2014. RAxML version 8: A tool for phylogenetic analysis and post-analysis of large phylogenies. Bioinformatics 30, 1312–1313. https://doi.org/10.1093/bioinformatics/btu033.
Stamatakis, A., Hoover, P., Rougemont, J., 2008. A rapid bootstrap algorithm for the RAxML web servers. Syst. Biol. 57, 758–771. https://doi.org/10.1080/10635150802429642
Stange, M., Sánchez-Villagra, M.R., Salzburger, W., Matschiner, M., 2018. Bayesian divergence-time estimation with genome-wide single-nucleotide polymorphism data

of sea catfishes (Ariidae) supports miocene closure of the Panamanian Isthmus. Syst. Biol. 67, 681–699. https://doi.org/10.1093/sysbio/syy006
Steinfartz, S., Veith, M., Tautz, D., 2000. Mitochondrial sequence analysis of Salamandra taxa suggests old splits of major lineages and postglacial recolonizations of Central Europe from distinct source populations of Salamandra salamandra. Mol. Ecol. 9 (4), 397–410. https://doi.org/10.1046/j.1365-294x.2000.00870.x.
Tiley, G.P., Poelstra, J.W., dos Reis, M., Yang, Z., Yoder, A.D., 2020. Molecular Clocks without Rocks: New Solutions for Old Problems. Trends Genet. 36 (11), 845–856. https://doi.org/10.1016/j.tig.2020.06.002.
Uotila, E., Crespo-Diaz, A., Sanz-Azkue, I., Rubio, X., 2013. Variation in the reproductive strategies of Salamandra salamandra (Linnaeus, 1758) populations in the province of Gipuzkoa (Basque Country). Munibe 61, 91–101.
Veith, M., Steinfartz, S., Zardoya, R., Seitz, A., Meyer, A., 1998. A molecular phylogeny of 'true'salamanders (family Salamandridae) and the evolution of terrestriality of reproductive modes. J. Zool. Syst. Evol. Res. 36, 7–16. https://doi.org/10.1111/j.1439-0469.1998.tb00774.x.
Velo-Antón, G., García-París, M., Galán, P., Cordero Rivera, A., 2007. The evolution of viviparity in holocene islands: Ecological adaptation versus phylogenetic descent along the transition from aquatic to terrestrial environments. J. Zool. Syst. Evol. Res. 45 (4), 345–352. https://doi.org/10.1111/jzs.2007.45.issue-410.1111/j.1439-0469.2007.00420.x.
Velo-Antón, G., Lourenço, A., Galán, P., Nicieza, A., Tarroso, P., 2021. Landscape resistance constrains hybridization across contact zones in a reproductively and morphologically polymorphic salamander. Sci. Rep. 11, 1–16. https://doi.org/10.1038/s41598-021-88349-7.
Velo-Antón, G., Santos, X., Sanmartín-Villar, I., Cordero-Rivera, A., Buckley, D., 2015. Intraspecific variation in clutch size and maternal investment in pueriparous and larviparous Salamandra salamandra females. Evol. Ecol. 29 (1), 185–204. https://doi.org/10.1007/s10682-014-9720-0.
Velo-Antón, G., Zamudio, K.R., Cordero-Rivera, A., 2012. Genetic drift and rapid evolution of viviparity in insular fire salamanders (Salamandra salamandra). Heredity (Edinb). 108 (4), 410–418. https://doi.org/10.1038/hdy.2011.91.
Vences, M., Sanchez, E., Hauswaldt, J.S., Eikelmann, D., Rodríguez, A., Carranza, S., Donaire, D., Gehara, M., Helfer, V., Lötters, S., Werner, P., Schulz, S., Steinfartz, S., 2014. Nuclear and mitochondrial multilocus phylogeny and survey of alkaloid content in true salamanders of the genus Salamandra (Salamandridae). Mol. Phylogenet. Evol. 73, 208–216. https://doi.org/10.1016/j.ympev.2013.12.009.
Wake, M.H., 2015. Fetal adaptations for viviparity in amphibians. J. Morphol. 276 (8), 941–960. https://doi.org/10.1002/jmor.v276.810.1002/jmor.20271.
Wake, M.H., 1982. Diversity within a framework of constraints. Amphibian reproductive modes, in: Environmental Adaptation and Evolution. Gustav Fischer New York, USA, pp. 87–106.
Weisrock, D.W., Hime, P.M., Nunziata, S.O., Jones, K.S., Murphy, M.O., Hotaling, S., Kratovil, J.D., 2018. Surmounting the Large-Genome "Problem" for Genomic Data Generation in Salamanders, in: Population Genomics: Wildlife. pp. 1–28. https://doi.org/10.1007/13836_2018_36